Global NEST Journal, Vol 27, No 4, 06944

Study on the removal and adsorption kinetics of malachite green in water by NaY molecular sieve prepared from coal gangue

Qingping Wang[1,2,3], Jing Min[1] and Wei Xu[1]
[1]School of Materials Science and Engineering, Anhui University of Science and Technology, Huainan 232001, China
[2]Anhui Industrial Generic Technology Research Center for New Materials from Coal-Based Solid Wastes, Anhui University of Science and Technology, Huainan 232001, China
[3]State Key Laboratory of Mining Response and Disaster Prevention and Control in Deep Coal Mines, Anhui University of Science and Technology, Huainan 232001, China
Received: 31/10/2024, Accepted: 05/02/2025, Available online: 18/02/2025
*to whom all correspondence should be addressed: e-mail: wqp.507@163.com
https://doi.org/10.30955/gnj.06944

Graphical abstract

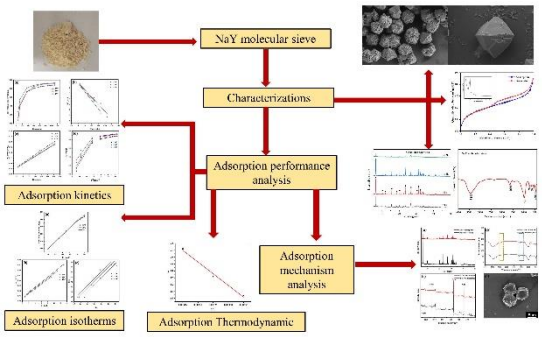

Abstract

The synthesis of NaY molecular sieve from coal gangue and its adsorption properties for malachite green were studied. The process adopts high-temperature sintering hydrothermal method, which not only improves the utilization rate of coal gangue, but also analyzes the key parameters affecting the formation of molecular sieve with high adsorption efficiency of organic pollutants, and characterizes the materials by XRD, SEM, EDS, BET, etc. The adsorption process of malachite green solution was analyzed by adsorption kinetics and isotherm, and the adsorption mechanism was elucidated by XRD, FTIR, XPS and SEM. The results show that the maximum adsorption capacity of NaY molecular sieve for malachite green is 1910mg/g under the best conditions, which conforms to the quasi-second-order kinetic equation and Langmuir isothermal adsorption model.

Keywords: gangue, NaY molecular sieve, hydrothermal method, MG adsorption

1. Introduction

Water pollution has always been a major issue of global concern, especially printing and dyeing wastewater containing organic dyes (Dhaouefi *et al.* 2022). Malachite green (MG), as a typical alkaline and cationic dye, has a strong bactericidal ability, and even at lower concentrations it can act as a good inhibitor of bacteria (Guo *et al.* 2020), which is widely used in the aquaculture industry (Gavrilenko *et al.* 2019). However, due to the continuous accumulation of MGs in water bodies, they can damage water ecosystems, jeopardize the safety of water resources and affect the stability of aquatic ecosystems (Lin *et al.* 2022).To remove this toxic dye, various adsorption methods have been investigated, including photocatalytic oxygenation (Aswathy, JiJi, and Kumar 2022), chemical precipitation (Wang *et al.* 2022), adsorption (Gong *et al.* 2021). Among them, the adsorption method is considered as one of the most effective routes due to its ease of operation, absence of secondary pollution, and high removal rate (Shi *et al.* 2017) Adsorption. Kezhou Yuan *et al.* (Yan *et al.* 2023) A magnetic adsorbent made of CG was used to treat heavy metal ions in gold industry wastewater. It was found that the rate of adsorption of heavy metals Pb(II), Cd(II) and Cu(II) by this magnetic material was more than 70%. Hao Zhang et al (Zhang *et al.* 2022) synthesized ammonium Phosphotungstic /CG (NH4-PW/CG) through a simple precipitation method using gangue as the carrier. The adsorption efficiency of ciprofloxacin (CIP) exceeded 82% within 10 minutes. Xue Ma et al (Ma *et al.* 2023) prepared ZSM-5/CLCA molecular sieves from gangue using cellulose aerogel (CLCA) as the raw material and cellulose aerogel (CLCA) as the green templating agent using hydrothermal method. By studying the optimal conditions and reaction mechanism of product synthesis, it was proved that the material had good adsorption performance for malachite green, and the adsorption amount was 136.5 mg/g.

Coal gangue is a type of solid waste generated during coal mining and coal washing processes. It's a rock with a dark grey color. low carbon content and harder than coal, and it is an important solid waste for the development and utilization of China's coal resources, accounting for about 15-20% of the total amount of raw coal((Zheng *et al.* 2024). In recent years, with the rapid growth of China's economy and the surging demand for coal power, China

has been the world's largest coal producer and consumer (Haibin and Zhenling 2010) The amount of coal gangue stockpiles has exceeded 5 billion tones. The accumulation of large amounts of coal gangue has resulted in the depletion of land resources, causing landslides, mudslides and other geological disasters, and bringing many adverse effects on local water, soil and air (Ge *et al.* 2020), It also poses a great threat to human health (Yun *et al.* 2016). The accumulation of the rock has caused the depletion of land resources and the occurrence of geological disasters such as landslides and mudslides, which have brought many adverse effects on the local water, soil and air. In recent years, researchers have been exploring and practice the use of coal gangue. Currently, people use coal gangue as mine backfill, road additives, and also made into agricultural fertilizer and flocculant (Gao *et al.* 2023). The gangue is also used in the fields of power generation, building materials production and land reclamation (Wu *et al.* 2024). However, this "low value-added" utilization has once again caused the waste of mineral resources (Li and Wang 2019). How to achieve high value-added use of coal gangue has become a hot research topic. Under China's current environmental protection strategy, this is one of the green upgrades urgently needed by the industry. Synthesis of zeolite molecular sieve from gangue as raw material will be one of the new uses of gangue.

Na-Y molecular sieves were synthesized for environmental remediation using an alkali-soluble hydrothermal method with coal gangue as the primary material. This approach not only significantly reduced waste emissions but also enhanced the overall utilization of solid waste. The study explored the potential of producing Na-Y molecular sieves from coal gangue, which is rich in silicon and aluminum, and experimentally determined the optimal parameters for their synthesis.To understand the adsorption mechanisms of the molecular sieves on contaminants, various adsorption experiments were conducted. These included tests on different conditions, such as molecular sieve concentration and pH levels, as well as the application of adsorption kinetic models.

2. Experimental

2.1. Experimental reagents

The gangue sourced from Huainan City, Anhui Province, China, served as the aluminum and silicon sources for the experiments. Sodium hydroxide (NaOH, AR, ≥99.70%) was procured from Sinopharm Chemical Reagent Co. Ltd, The pure water used in the experiment was self-made deionized water. All reagents employed in this study were of analytical grade and did not undergo any pretreatment experimental methodology.

2.2. Preparation of molecular sieves

Nay molecular sieves were synthesized via a conventional hydrothermal method, as illustrated in Figure 1. Initially, gangue was calcined at 850 °C in an open ceramic crucible. After reaching the desired roasting temperature, the crucible was left in the furnace for 2 h and then cooled to room temperature. Subsequently, the calcined gangue was uniformly mixed with NaOH in a ball milling jar at a mass ratio of 1:1.2. The mixture was then subjected to further calcination at 500 °C for 2 h to obtain the alkali-soluble product, as depicted in steps (1) and (2) of the alkali-soluble process (Kong and Jiang 2021) :

$$SiO_2 + 2NaOH = Na_2SiO_3 + H_2O \quad (1)$$

$$Al_2O_3 \cdot 2SiO_2 + 2NaOH = 2NaAlSiO_4 + H_2O \quad (2)$$

Following this, 6.59 g of alkali-soluble product, 0.84 g of hydroxide, and 60 ml of deionized water were sequentially added to a beaker and age at 45 degrees for 10 h. After thorough aging, the raw material was transferred into a stainless steel container lined with polytetrafluoroethylene and placed in an oven at 80 °C for 10 h. Finally, the sample was cooled, filtered, washed to neutrality, and dried in a vacuum drying oven at 100 °C for 6 h.

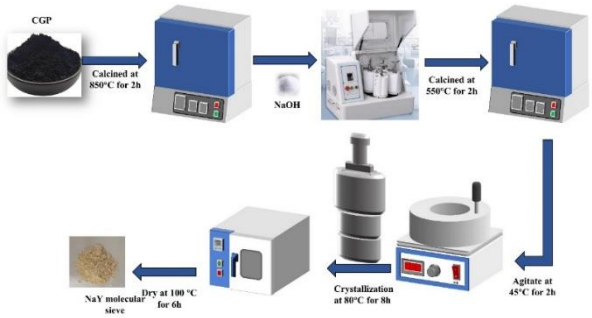

Figure 1. Process flow diagram of Nay molecular sieve synthesis from gangue.

2.3. Adsorption eExperiment of MG

20 mg of MG powder was added to a 250 ml beaker, followed by filling with 100 ml of deionized water and stirring at 500 rpm for 0.5 h in a thermostatic water tank to ensure complete dissolution of the MG. After dissolution, the solution was transferred to a 1 L volumetric flask to determine the volume, resulting in an MG stock solution of 200 mg/L. The absorbance of the solution was measured at 617 nm by UV-VIS spectrophotometer. The MG standard curve is shown in Figure 2.

The prepared molecular sieve was used for the adsorption test of MG。 After adsorption, the adsorbent is separated from the MG solution using a high-speed centrifuge. The absorbance of the solution before and after adsorption was recorded by UV-VIS spectrophotometer. The formulas for calculating the adsorption capacity and removal rate of dyes are shown in (3):

$$Q_e = \frac{(C_0 - C_e)*V}{W} \quad (3)$$

In the formula. Q_e is the adsorption capacity (mg/L); C_0, C_e are the concentration of MG in solution before and after adsorption (mol/L), respectively; V is the volume of MG in the experiment; *W* is the amount of molecular sieve (g); *n* is the removal rate of MG in solution.

2.4. Characterization

The raw material composition and content of coal gangue were analyzed by ARL-9800 X-ray fluorescence

spectroscopy (XRF). The crystal patterns and characteristics of the samples were analyzed by Shimadzu XRD-6000 X-ray diffractometer. The micromorphology of the samples was analyzed using an electron microscope (SEM, ZSISS Sigma 300), and the surface elements were analyzed by energy dispersive spectrometry (EDS). Bruker's IFS88 Fourier transform infrared spectrometer FT-IR was used to analyze the functional groups of the samples, and the wave number was selected in the range of 4000-400cm^{-1}. X-ray electron spectroscopy (XPS) of ESCALB Xi^{+} was used to study the adsorption mechanism. Finally, at −196℃, the N_2 adsorption-desorption isotherm of the sample was determined using the Micromeritics ASAP 2020 analyzer (Micromeritics, Norcross, GA, USA) to assess its surface area and pore size.

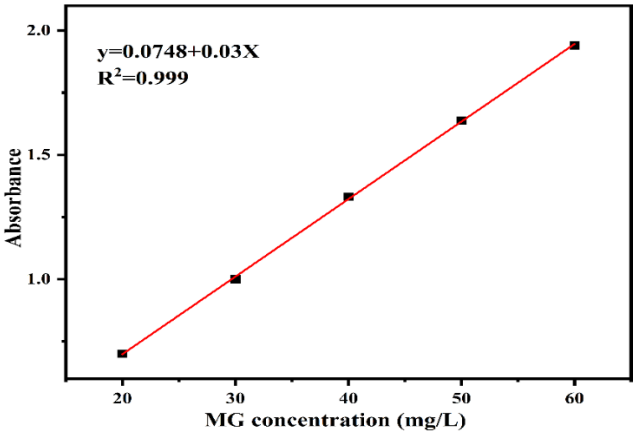

Figure 2. MG standard curve.

Table 1. Main chemical composition in gangue (wt.%)

SiO_2	Al_2O_3	Fe_2O_3	CaO	MgO	NaO_2	TiO_2	other than
55.62	30.43	6.37	2.47	1.05	0.9	0.92	2.24

Table 2. Surface structure parameters of NaY molecular sieve

	Specific surface area (BET) m² /g	Pore volume m³ /g	Particle stacking pore size nm
waste rock (in coal mining)	5.00	-	-
Nay molecular sieve	621.92	0.21	4.69

3. Results and discussion

3.1. Gangue analysis

The main chemical composition (wt.%) of the gangue was determined by X-ray fluorescence spectroscopy (XRF), and the results are presented in Table 1. Based on the wt.% values listed in Table 1, the molar ratio of SiO_2/Al_2O_3 in the gangue was calculated to be approximately 3.1. This ratio indicates that the gangue can serve as a source of pure silicon and aluminum for synthesizing Nay molecular sieves.

It can be seen from the XRD pattern (as shown in Figure 3) that the main mineral components of coal gangue are quartz and kaolinite, the structure is stable and the activity is low. Therefore, coal gangue raw material can not meet the raw material requirements for preparing Nay molecular sieve. Before the hydrothermal reaction, the coal gangue needs to be further activated.

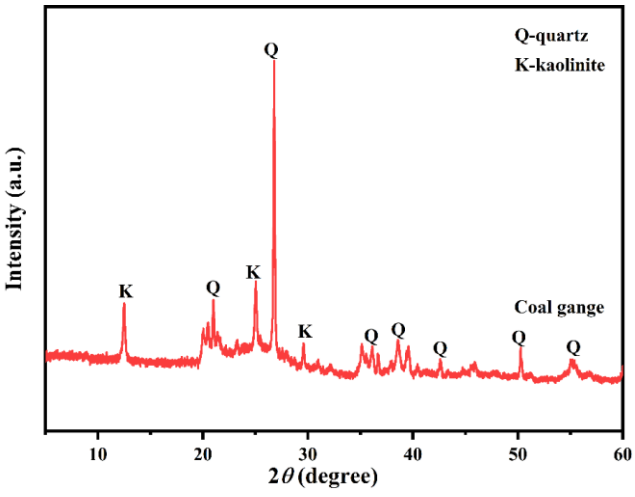

Figure 3. XRD spectra of gangue raw samples.

The X-ray diffraction (XRD) pattern of coal gangue following high-temperature calcination and alkali melting is illustrated in Figure 4. Analysis of this Figure reveals that the characteristic peak of kaolinite disappears during the alkali melting process. Additionally, the intensity of the quartz peak is notably reduced. In contrast, new crystalline phases such as muscovite, calcite, sodalite, and calcium ferrite emerge. These phases exhibit higher reactivity, which enhances the potential for synthesizing molecular sieves in subsequent hydrothermal reactions.

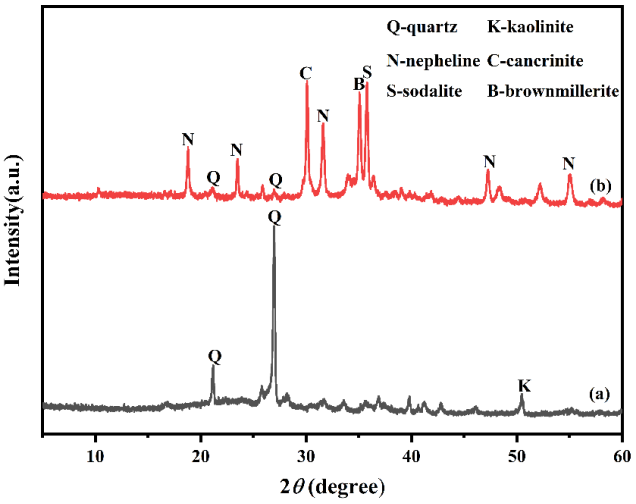

Figure 4. XRD pattern of coal gangue after calcination(a); XRD pattern of alkali dissolved coal gangue(b).

Scanning electron microscopy was used to analyze the microscopic morphology of coal gangue. As shown in Figure 5, it can be seen that coal gangue raw materials are irregular lumps or aggregates with uneven particle size distribution and significant amorphous particulate matter appearing on the surface.

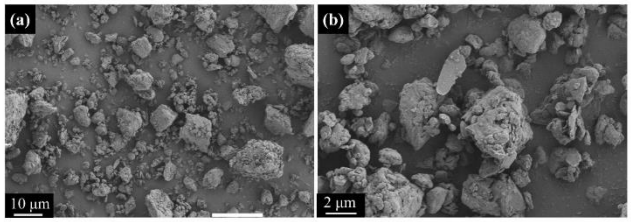

Figure 5. SEM image of gangue original sample.

3.2. Effect of preparation conditions on the synthesis of Nay molecular sieves

3.2.1. Effect of crystallization temperature

In this phase, XRD analysis was conducted on Nay molecular sieves synthesized at various crystallization temperatures over a period of 8 hours, as shown in Figure 6. At lower temperatures, the energy available for the reaction is limited, resulting in minimal formation of crystalline phases in the synthetic products. In a closed reactor, fluctuations in crystallization temperature can cause pressure changes, which in turn affect the nucleation and growth processes of the sample, leading to variations in the crystallization product's structure. Figure 6 indicates that once the reaction temperature exceeds 80 °C, both the characteristic diffraction peak and the overall crystallinity of the synthesized product start to decline as the temperature rises. Additionally, the emergence of other crystal types on the surface of the product and the formation of nerite are observed at these higher temperatures. Therefore, the optimal crystallization temperature is identified as 80 °C.

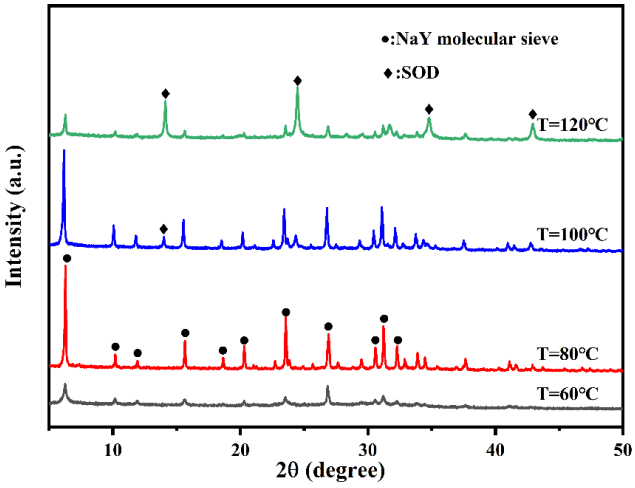

Figure 6. XRD patterns of Nay molecular sieves synthesized at differentcrystallization temperatures.

3.2.2. Effect of crystallization time crystallization

The XRD patterns of Nay zeolite synthesized at 80 °C with varying crystallization times are depicted in Figure 7. It is evident from Figure 7 that the intensity of the diffraction peaks of the synthesized sample is highest when the crystallization time is 8 h. Additionally, the characteristic diffraction peak of the create sample corresponds to the diffraction peak of the standard PDF card 43-0168, indicating that the synthesized sample at this crystallization temperature is a typical Nay molecular sieve.

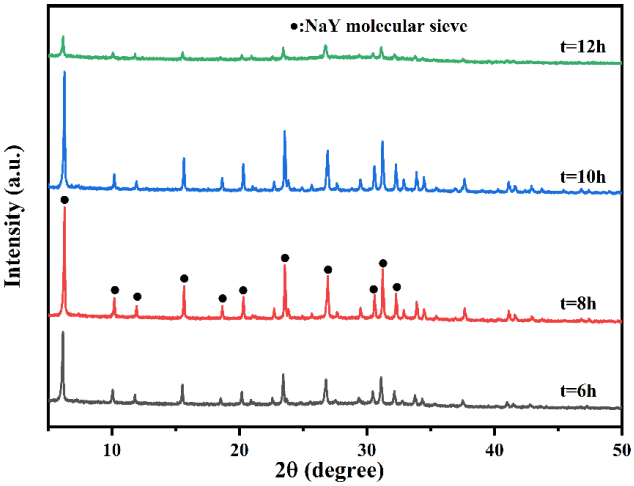

Figure 7. XRD patterns of Nay molecular sieves synthesized at different crystallization times.

3.3. Scanning analysis

In Figures 8 (a ~ d), SEM images show the development of Na-Y zeolite at various crystallization times. The images reveal that octahedral nuclei of the Na-Y molecular sieve begin to form at different time intervals. At the 6-hour mark, some unreacted raw materials are still visible. However, after extending the crystallization time to 8 hours, the sample exhibits a well-defined octahedral structure with a smooth and intact surface, measuring approximately 2 μm in size. Figure 9 presents the surface composition of the prepared Na-Y molecular sieve, analyzed through SEM-EDS. The distribution of elements—silicon, aluminum, sodium, and oxygen—appears uniform across the surface of the molecular sieve. The EDS spectrum further confirms the presence of these main elements, providing consistency in the analysis.

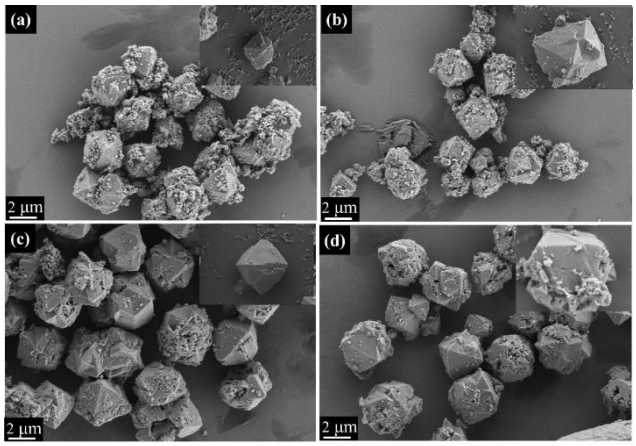

Figure 8. SEM images of synthesized Nay molecular sieves with different crystallization times:(a) 6 h; (b) 8 h; (c) 10 h; (d) 12 h.

3.4. FT-IR analysis

The infrared spectrum of NaY molecular sieve is shown in Figure 10. In the synthesized products, characteristic absorption peaks near 1656 cm^{-1} and 991 cm^{-1} represent the O-H bending vibration of water molecules and the asymmetric stretching vibration of Si-O bonds, respectively. The absorption peak near 752 cm^{-1} is attributed to the stretching mode of tetrahedral atoms, while the peak near 667 cm^{-1} corresponds to the Al-O symmetric stretching vibration. Furthermore,

characteristic absorption peaks arising from double hexagonal ring vibrations are noted around 565 cm^{-1} when Al is in an octahedral coordination state (Rao *et al.* 2023), and the bending vibration of the tetrahedral Si-O-Al chain leads to characteristic peaks near 458 cm^{-1}. These findings confirm the successful conversion of gangue into Nay molecular sieves, as evidenced by characterization techniques including X-ray diffraction, scanning electron microscopy, and infrared spectroscopy.

3.5. Specific surface area analysis

BET specific surface area analysis is a widely used method for characterizing the pore structure of solid materials, based on the adsorption of gases on solid surfaces. This analysis uses adsorption isotherm data to examine the material's pore structure. According to Table 2, the specific surface area of gangue is only 5.0 m^2/g, suggesting that the raw gangue material has a very weak adsorption capacity. Conversely, the BET specific surface area of the Nay molecular sieve, synthesized through a hydrothermal reaction, reaches 621.92 m^2/g with an average pore size of 4.69 nm. The BJH curve depicted in Figure 11b shows that the Nay zeolite possesses a microporous and mesoporous structure, with the pore size predominantly concentrated around mesopores of 4.69 nm. According to the IUPAC classification standards, the isotherm curve of the Nay molecular sieve can be categorized as a Type IV curve, primarily characteristic of mesoporous materials. This type of isotherm reflects multilayer adsorption on the surfaces of non-porous homogeneous solids and is indicative of a typical physical adsorption process.

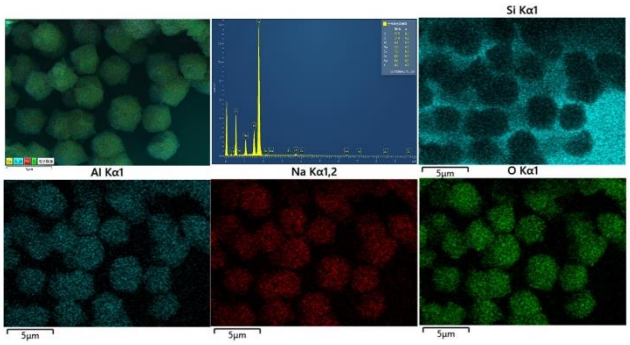

Figure 9. EDS spectra of Nay molecular sieve.

Table 3. Fitting parameters of adsorption kinetics.

Kinetic models	Parameters	Temperature 25 °C, 35 °C, 45 °C		
	$q_{e.ecp}$	1877	1890	1910
quasi-first-orde	q_{e1} (mg/g)	1099	940	900
	k_1 (min^{-1})	0.0053	0.0054	0.0062
	R^2	0.9558	0.9929	0.9819
Pseudo-second-order	q_{e2} (mg/g)	1960	1988	1990
	k_2 (g/(mg·min))	0.00011	0.000113	0.00015
	R^2	0.999	0.999	0.999
Intra-particle Diffusion	K_{t1}(mg/(g/min)$^{1/2}$)	54.43	53.13	45.79
	C_1	777	779	971
	R_1^2	0.8857	0.9006	0.8730
	K_{t2}(mg/(g/min)$^{1/2}$)	6.22	5.62	4.46
	C_2	1660	1722	1772
	R_2^2	0.9556	0.8298	0.9549

3.6. Adsorption performance analysis

3.6.1. Adsorption kinetics

The adsorption process of MG by NaY molecular sieve can be described by quasi-first-order (Eq.(4)), quasi-second-order (Eq.(5)) and intra-particle diffusion model (Eq.(6)).

$$ln(q_e - q_t) = \ln q_e - k_1 t \quad (4)$$

$$\frac{t}{q_t} = \frac{1}{K_2 q_e^2} + \frac{1}{q_e} t \quad (5)$$

$$q_t = k_t t^{\frac{1}{2}} + C \quad (6)$$

In the formula, q_e and q_t are respectively the adsorption capacity of MG at 1380 (min) and the adsorption capacity of t (min) time (mg/g); k_1 (min^{-1}), k_2[g/(min·mg)] and kid[mg/ (g/$min^{1/2}$)] are the rate constants of the quasi-first-order kinetic equation, the quasi-second-order kinetic equation and the rate of intra particle diffusion, respectively. C is the adsorption constant; t is the adsorption time (min).

In order to investigate the adsorption rate of NaY molecular sieve for MG, 10 MG NaY molecular sieve was added to 100 mL MG solution with a concentration of 200 MG /L. Adsorption rates were measured at temperatures of 25°C, 35°C and 45°C. As shown in Figure 12a, the adsorption rate gradually decreases with the increase of adsorption time, while the adsorption rate and capacity increase with the increase of temperature. The kinetic fitting results are displayed in Figure 12b、c, and summarized in Table 3. As indicated in Table 3, the correlation coefficients of the pseudo-second-order kinetic model are significantly higher than those of the pseudo-first-order model across all temperatures. Moreover, the saturation adsorption capacities predicted by the pseudo-second-order model align more closely with the experimental values, suggesting that the adsorption of MG onto the NaY molecular sieve at various temperatures follows a pseudo-second-order kinetic model. This implies that the primary adsorption mechanism is chemisorption (Meena, Kukreti, and Jassal 2024). As shown in Figure 12d, all fitted curves appear as

straight lines that do not pass through the origin, indicating that the intercept C is not equal to zero. Additionally, Table 3 shows that while the fitted curves exhibit a strong linear relationship, they do not intersect the origin. These observations suggest that, beyond internal diffusion, multiple mechanisms influence the adsorption of MG onto the molecular sieve (Li *et al.* 2023).

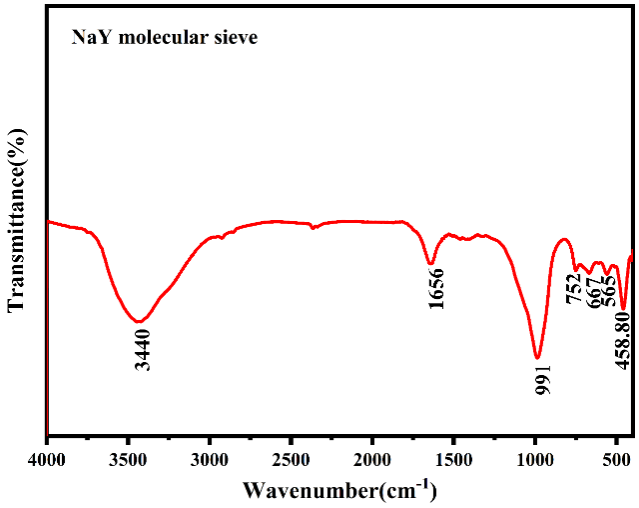

Figure 10. FT-IR spectra of Nay molecular sieves.

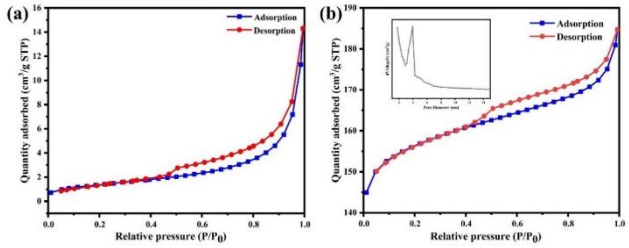

Figure 11. N2 adsorption-desorption isotherm curve of coal gangue(a); N2 adsorption-desorption isotherm curve and pore size distribution of NaY molecular sieve(b).

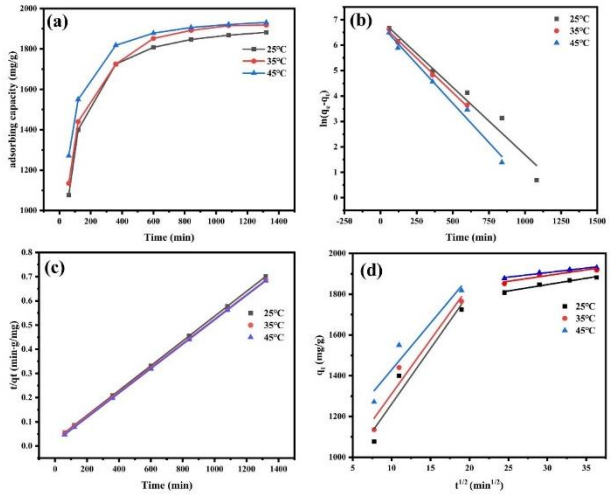

Figure 12. the impact of time on MG (a) ;Quasi-first-order kinetic curve(b) ;Quasi-second-order kinetic curve (c); Intraparticle diffusion model curve(d).

3.6.2. Adsorption isotherms

The adsorption data were simu-ated with the Langmuir model (Eq. (7)) (Mahreni *et al.* 2022)and the Freundlich model (Eq. (8)) (Uyiosa Osagie *et al.* 2021).

$$\frac{C_e}{q_e} = \frac{C_e}{q_{max}} + \frac{1}{K_L q_{max}} \quad (7)$$

$$lnq_e = lnK_f + \frac{1}{n} lnC_e \quad (8)$$

Where q_{max} (mg/g) means maximum saturated adsorption amount, K_L (L/mg) refers to the Langmuir constant, K_F (mg/g) represents the adsorption coefficient and 1/n means Freundlich constants.

To evaluate the isothermal adsorption process, 10 mg of NaY molecular sieve was introduced into 100 mL of MG solution at varying concentrations. The equilibrium adsorption behavior was examined at temperatures of 25°C 、 35°C, and 45°C. Figure 13a illustrates the adsorption isotherms of the NaY molecular sieve for MG across different temperatures and concentrations, offering insights into the adsorption characteristics under these conditions. Figure 13b and c present the analysis of adsorption behavior using the Langmuir and Freundlich isotherm models, with the derived parameters detailed in Table 4. For NaY molecular sieve, the adsorption capacity increased as the initial concentration of MG rose, and showed a slight enhancement with elevated temperatures. The increase in adsorption at higher temperatures suggests that the adsorption of MG onto NaY zeolite is an endothermic process. The fitting correlation coefficients R^2 (0.9967、0.9923、0.9990) of the Langmuir isothermal model at different temperatures were higher than those of the Freundlich isothermal adsorption model,. This suggests that the adsorption of MG onto the NaY molecular sieve follows a monolayer adsorption mechanism. While the Freundlich isotherm model can describe the adsorption process in certain scenarios, the Langmuir model exhibits a stronger correlation with the NaY molecular sieve data in this experiment, providing a more accurate interpretation of the adsorption behavior. In addition, Table 5 shows the comparison of adsorption of MG by different adsorbents synthesized from solid wastes. It can be seen that the NaYmolecular sieve synthesized from solid waste has a high specific surface area and good MG adsorption performance. However, there is no research on synthesizing NaYmolecular sieve for MG adsorption using coal gangue. Additionally, Table 5 presents a comparison of MG adsorption performance by various adsorbents derived from solid wastes. It is evident that the NaY molecular sieve synthesized from solid waste exhibits a high specific surface area and excellent MG adsorption capacity. However, there is a lack of studies on the use of coal gangue to synthesize NaY molecular sieves for MG adsorption.

3.6.3. Adsorption thermodynamic model

The thermodynamics of adsorption is typically analyzed using key thermodynamic parameters, such as enthalpy change (△H), entropy change (△S), and Gibbs free energy (△G). These functions provide valuable insights into the nature and feasibility of the adsorption process. The calculation formula is shown in equation (9)、 (10)、(11) and (12) :

$$K_c = C_{\alpha,e} / C_e \quad (9)$$

$$\Delta G = RT\ln K_c \quad (10)$$

$$\Delta G = \Delta H - T\Delta S \quad (11)$$

$$\ln K_c = -\frac{\Delta H}{RT} + \frac{\Delta S}{R} \quad (12)$$

Where Kc represents the adsorption coefficient, Ce is the equilibrium concentration of MG molecules in the solution (mg/g), and Ca,e denotes the concentration of MG molecules on the adsorbent at equilibrium (mg/g). T is the absolute temperature (K), and R is the ideal gas constant, valued at 8.314 J/(mol·K). ΔH (enthalpy change, kJ·mol^{-1}), ΔS (entropy change, kJ·mol^{-1}), and ΔG (Gibbs free energy, kJ·mol^{-1}).

Table 4. The parameters of adsorption isotherms.

Kinetic models	Parameters	Temperature 25 °C, 35 °C, 45 °C		
Langmuir model	q_m (mg/g)	2078	2106	2123
	K_L(L/mg)	0.6687	0.7683	0.9942
	R_2	0.9967	0.9923	0.9990
Freundlich model	K_F (mg/g)	940	1050	1100
	1/n	0.2801	0.2721	0.2698
	R^2	0.9653	0.9592	0.9519

Table 5.Summary of literature on the specific surface area and MG adsorption of ad-sorbents synthesized from solid wastes.

Raw	Adsorbent	Specific surface are (m^2g^{-1})	Adsorption capacity (mg g^{-1})	Reference
Coal gasification slag	ZSM-5	299	80	(Yuan *et al.* 2022)
Fly ash	Flyash molecular sieve	404	32	(Zgureva *et al.* 2020)
Coal gangue	ZSM-5	398	136.5	(Ma *et al.* 2023)
Metakaolin	Zeolite A	/	55	(Pereira *et al.* 2018)

Table 6. Nay-type molecular sieve adsorption of MG thermodynamic parameters.

Temperature (°C)	Thermodynamic fitting parameters		
	△H （kJ/mol）	△S （J/(mol•K)）	△G （kJ/mol）
25	-	-	-34.5
35	284.3	1070	-45
45	-	-	-55

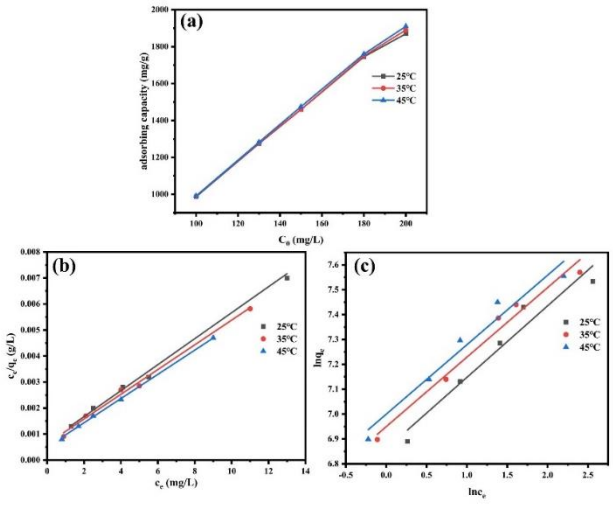

Figure 13. Adsorption isotherm of NaY molecular sieve to MG (a) ;Langmuir model (b) and Freundlich model(c).

By plotting lnKd and 1/ T and performing linear fitting on the experimental data, Figure 14 was generated. Table 5 presents the calculated values of ΔG, ΔS and ΔH, and further interprets the direction, extent, and feasibility of MG adsorption based on their signs. As shown in Table 5, the positive value of ΔH>0 suggests that the adsorption process is endothermic. The negative values of ΔG across different temperatures indicate that the adsorption of MG by the molecular sieve is spontaneous. Furthermore, the decrease in ΔG with rising temperature implies that higher temperatures enhance the spontaneity of the process, thus favoring adsorption. The positive value of ΔS>0 suggests an increase in disorder within the reaction system, which further facilitates the adsorption of MG onto the NaY molecular sieve.

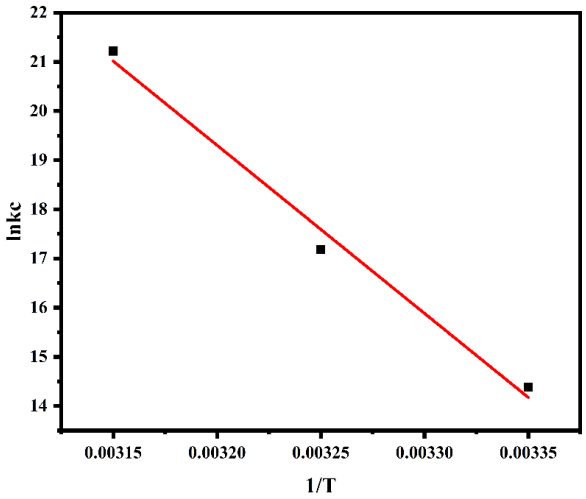

Figure 14. Thermodynamic fitting diagram of adsorption of MG by NAY-type molecular sieve.

3.7. Adsorption mechanism analysis

The adsorption mechanism of NaY molecular sieve on MG was studied by XRD, FT-IR, XPS and SEM. As can be seen from Figure 15a, the intensity of XRD diffraction peaks was significantly weakened after MG adsorption by the

molecular sieve, while the typical X-ray diffraction peaks corresponding to NaY molecular sieve remained intact, indicating that the crystal structure of the molecular sieve was not destroyed after MG adsorption. FT-IR spectra of NaY molecular sieve before and after adsorption were given (Figure 15b). It can be seen from Figure 15b that the characteristic peaks of MG dye molecules appear in the FT-IR spectra of 1600-1300−1 and 2800-3000−1 after adsorption, which proves that MG is adsorbed on the surface of the material. XPS analysis was performed on the molecular sieve before and after adsorption, and the results were shown in Figure 15c. It can be seen that after MG adsorption, the characteristic peaks of Mg1s and Na1s at 1303.10eV almost disappear, indicating that the adsorption of MG is caused by ion exchange, mainly the exchange of dye cation and Na+. The morphologies of adsorbed samples were observed by scanning electron microscopy (SEM). The SEM image of the Nay-type molecular sieve after adsorption of MG shown in Figure 15d shows that the original particle structure of the molecular sieve is basically intact, which is consistent with the peak shape retention observed in the XRD pattern of Figure 15a. However, the surface becomes noticeably rough, with many fine sheets of material attached to the previously smooth octahedral particles. These deposits may be MG dyes, further confirming that Nay-type molecular sieve successfully adsorbed dye molecules.

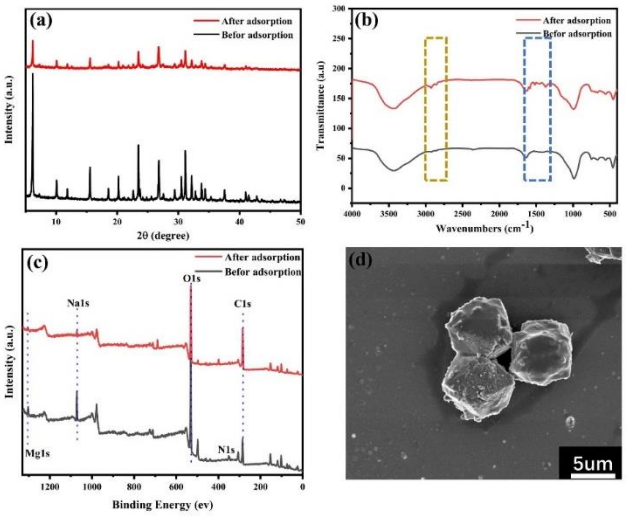

Figure 15. XRD (a), FT-IR (b), and XPS (c) analyses of the NaY molecular sieve before and after adsorption; SEM image of molecular sieve after adsorption (d).

4. Conclusion

The successful synthesis of NaY molecular sieve from coal gangue provides an effective way to increase the added value of solid waste and deal with environmental problems. Through the optimized hydrothermal process and alkali activation, the NaY molecular sieve obtained has a specific surface area of 621.92 m^2/g and an average pore size of 4.69 nm, which makes it excellent in the removal of malachite green, and the maximum adsorption capacity reaches 1910 mg/g. The adsorption process follows the pseudo-second-order kinetic model and is in good agreement with the Langmuir isothermal model, which indicates that the main adsorption mechanism is chemisorption. The thermodynamic results show that the adsorption of MG is a spontaneous endothermic process. XRD、FT-IR and XPS analysis proved that chemisorption (ion exchange) was the main mechanism of NaY molecular sieve adsorption of malachite green. These studies highlight the potential for synthesizing high-performance adsorbents from coal gangue to not only help reduce waste, but also aid in the remediation of contaminated water sources. Future work could explore scaling up the process and testing the material's effectiveness in real-world applications, which could lead to broader environmental benefits.

Author contributions

All authors have contributed to the study conception and design. “Conceptualization, Jing Min and Qingping Wang; validation, Wei Xu; investigation, Jing Min; data curation, Jing Min; writing—original draft, Jing Min; supervision, Qingping Wang; project administration, Qingping Wang. All authors have read and agreed to the published version of the manuscript.”

Acknowledgments

This research was funded by National Natural Science Foundation of China (NSFC) [52227901]; the University Synergy Innovation Program of Anhui Province [GXXT-2022-083], [GXXT-2023-019]; Anhui Provincial Natural Science Foundation [2208085ME103].

References

Aswathy N. R., Varghese JiJi and Vinod Kumar R. (2022). 'Photocatalytic degradation of malachite green using vanadium pentoxide-doped NiO thin film by sol–gel spin coating', *The European Physical Journal Plus*. http://dx.doi.org/10.1007/s10653-021-01187-4

Dhaouefi, Zaineb, Aida Lahmar, Rihab Khlifi, Imene Ben Toumia, Dorra Elgueder and Leila Chekir-Ghedira. (2022). 'Evaluation of eventual toxicities of treated textile wastewater using anoxic–aerobic algal–bacterial photobioreactor', *Environmental Geochemistry and Health*. http://dx.doi.org/10.1016/j.matchemphys.2019.122240

Gao J., Lin Q., Yang T., Bao Y. C. and Liu J. (2023). 'Preparation and characterization of ZSM-5 molecular sieve using coal gangue as a raw material via solvent-free method: Adsorption performance tests for heavy metal ions and methylene blue', *Chemosphere*, 341: 139741. https://dx.doi.org/10.1016/j.chemosphere.2023.139741

Gavrilenko, N. A., Volgina T. N., Pugachev E. V. and Gavrilenko M. A. (2019). 'Visual determination of malachite green in sea fish samples', *Food Chem*, 274, 242–45. https://dx.doi.org/10.1016/j.foodchem.2018.08.139

Ge, Q., M. Moeen, Q. Tian, J. Xu and K. Feng. (2020). 'Highly effective removal of Pb(2+) in aqueous solution by Na-X zeolite derived from coal gangue', *Environmental Science and Pollution Research*, 27, 7398–408. https://dx.doi.org/10.1007/s11356-019-07412-z.

Gong, Liang, Jie Wang, Chenhao Jiang, Teng Xiao, Kang Shen, Ming Lei and Yiping Tang. (2021). 'Study on magnetic porous carbon microspheres as a novel adsorbent for malachite green', *ChemistrySelect,* https://dx.doi.org/10.1002/slct.202100129

Guo, Feiqiang, Xiaochen Jiang, Xiaolei Li, Xiaopeng Jia, Shuang Liang and Lin Qian. (2020). 'Synthesis of MgO/Fe3O4 nanoparticles embedded activated carbon from biomass for high-efficient adsorption of malachite green', *Materials Chemistry and Physics*, 240. https://dx.doi.org/10.1016/j.matchemphys.2019.122240.

Haibin, Liu, and Liu Zhenling. (2010). 'Recycling utilization patterns of coal mining waste in China', *Resources, Conservation and Recycling*, 54: 1331–40. https://dx.doi.org/10.1016/j.resconrec.2010.05.005.

Kong, Deshun and Rongli Jiang. (2021). 'Preparation of NaA Zeolite from High Iron and Quartz Contents Coal Gangue by Acid Leaching—Alkali Melting Activation and Hydrothermal Synthesis', *Crystals*. https://dx.doi.org/10.3390/cryst11101198

Li, Jiayan, and Jinman Wang. (2019). 'Comprehensive utilization and environmental risks of coal gangue: A review', *Journal of Cleaner Production*. https://dx.doi.org/10.1016/j.jclepro.2019.117946

Li, Wenlei, Huixin Jin, Hongyan Xie, Duolun Wang, and Ershuai Lei. (2023). 'Utilization of electrolytic manganese residue to synthesize zeolite A and zeolite X for Mn ions adsorption', *Journal of Industrial and Engineering Chemistry*, 120: 147–58. https://dx.doi.org/10.1016/j.jiec.2022.12.021

Lin, Yu-Ru, Yeh-Fang Hu, Chih-Yang Huang, Huai-Ting Huang, Zhen-Hao Liao, An-Ting Lee, Yu-Sheng Wu, and Fan-Hua Nan. (2022). 'Removing malachite green and leucomalachite green from freshwater and seawater with four water treatment agents', *Frontiers in Environmental Science*, 10. https://dx.doi.org/10.3389/fenvs.2022.906886.

Ma X., C. Ding H. Yang and Zhu X. (2023). Effects of a Cellulose Aerogel Template on the Preparation and Adsorption Properties of Coal Gangue-Based Multistage Porous ZSM−5. *Materials*. http://dx.doi.org/10.3390/ma16113896

Ma, X., C. Ding, H. Yang and X. Zhu. (2023). 'Effects of a Cellulose Aerogel Template on the Preparation and Adsorption Properties of Coal Gangue-Based Multistage Porous ZSM-5', *Materials*, 16. https://dx.doi.org/10.3390/ma16113896

Mahreni, Mahreni, Reza Rifky Ramadhan, Muhammad Fadhil Pramadhana, Annisa Putri Permatasari, Dini Kurniawati and Heri Septya Kusuma. (2022). 'Synthesis of Metal Organic Framework (MOF) based Ca-Alginate for adsorption of malachite green dye', *Polymer Bulletin*. https://dx.doi.org/10.1007/s00289-022-04086-5.

Meena, Hari Mohan, Shrikant Kukreti, and Jassal P. S. (2024). 'Synthesis of a novel chitosan-TiO2 nanocomposite as an efficient adsorbent for the removal of methylene blue cationic dye from wastewater', *Journal of Molecular Structure*. https://dx.doi.org/10.1016/j.molstruc.2024.139420

Pereira P., Ferreira B., Oliveira N., Nassar E., Ciuffi K., Vicente M., Trujillano R., Rives V., Gil A., Korili S. and de Faria E. (2018). Synthesis of Zeolite A from Metakaolin and Its Application in the Adsorption of Cationic Dyes. *Applied Sciences*. http://dx.doi.org/10.3390/app8040608

Rao, Zixin, Yu Chen, Kehui Qiu, Junfeng Li, Yu Jiao, Chengxiao Hu, Peicong Zhang and Yi Huang. (2023). 'Facile synthesis of NaY molecular sieve by low-temperature ultrasonic gelling method for efficient adsorption of rare-earth elements', *Materials Chemistry and Physics*, 293. https://dx.doi.org/10.1016/j.matchemphys.2022.126906

Shi, Zhennan, Ling Li, Yuxiang Xiao, Yingxi Wang, Keke Sun, Hangxing Wang and Li Liu. (2017). 'Synthesis of mixed-ligand Cu–MOFs and their adsorption of malachite green', *RSC Advances*. https://dx.doi.org/10.1039/c7ra04820c

Uyiosa Osagie, Aigbe, Ukhurebor Kingsley Eghonghon, Onyancha Robert Birundu, Osibote Otolorin Adelaja, Darmokoesoemo Handoko, and Kusuma Heri Septya. (2021). 'Fly Ash-based Adsorbent for Adsorption of Heavy Metals and Dyes from Aqueous Solution: A Review', *Journal of Materials Research and Technology*. https://dx.doi.org/10.1016/j.jmrt.2021.07.140

Wang, Li, Junbo Wang, Aishui Yu and Zuolong Yu. (2022). 'Removal of malachite green by electrochemical oxidation polymerization and electrochemical reduction precipitation: its kinetics and intermediates', *Journal of Solid State Electrochemistry*. https://dx.doi.org/10.1007/s10008-022-05242-7

Wu, Hao, Jingyi Yang, Lijinhong Huang, Wanfu Huang, Siyu Duan, Shangyuan Ji, Guixiang Zhang, Jun Ma and Jiushuai Deng. (2024). 'Full-components utilization: Study on simultaneous preparation of sodalite and separation of yttrium from coal gangue by chlorination roasting process', *Separation and Purification Technology*, 332. https://dx.doi.org/10.1016/j.seppur.2023.125802.

Yan, Kezhou, Jiyuan Zhang, Dandan Liu, Xiang Meng, Yanxia Guo and Fangqin Cheng. (2023). 'Feasible synthesis of magnetic zeolite from red mud and coal gangue: Preparation, transformation and application', *Powder Technology*. https://dx.doi.org/10.1016/j.powtec.2023.118495

Yuan, N., K. Tan, X. Zhang, A. Zhao and R. Guo (2022) Synthesis and adsorption performance of ultra-low silica-to-alumina ratio and hierarchical porous ZSM-5 zeolites prepared from coal gasification fine slag. *Chemosphere,* 303. http://dx.doi.org/10.1016/j.chemosphere.2022.134839

Yun, Yang, Rui Gao, Huifeng Yue, Xiaofang Liu, Guangke Li and Nan Sang. (2016). 'Polycyclic aromatic hydrocarbon (PAH)-containing soils from coal gangue stacking areas contribute to epithelial to mesenchymal transition (EMT) modulation on cancer cell metastasis', *Science of the Total Environment*. https://dx.doi.org/10.1016/j.scitotenv.2016.12.010

Zgureva D., Stoyanova V., Shoumkova A., Boycheva S. and Avdeev G. (2020). Quasi natural approach for crystallization of zeolites from different fly ashes and their application as adsorbent media for malachite green removal from polluted waters. *Crystals*. http://dx.doi.org/10.3390/cryst10111064

Zhang, Hao, Rongbo Zhao, Zhiliang Liu, Xiangchao Zhang and Chunfang Du. (2022). 'Enhanced adsorption properties of polyoxometalates/coal gangue composite:The key role of kaolinite-rich coal gangue', *Applied Clay Science*. https://dx.doi.org/10.1016/j.clay.2022.106730

Zheng, Qinwen, Yi Zhou, Xin Liu, Meng Liu, Libing Liao and Guocheng Lv. (2024). 'Environmental hazards and comprehensive utilization of solid waste coal gangue', *Progress in Natural Science: Materials International*. https://dx.doi.org/10.1016/j.pnsc.2024.02.012